Seasonal and Interannual Variations in Aerosol Characteristics at the ARM Southern Great Plains Site

M. Mahish[1], D. R. Collins[1], A. Jefferson[2], P. J. Marinescu[3], E. J. T. Levin[3], P. J. DeMott[3], and **S. M. Kreidenweis**[3]

[1]Texas A&M University, College Station, TX; [2]NOAA/ESRL, Boulder, CO; [3]Department of Atmospheric Science, Colorado State University, Fort Collins, CO

Abstract

Multiple years of aerosol data have been collected from routine observations at the ARM Southern Great Plains (SGP) site, along with specialized data from a number of intensive studies. More recently, the suite of routine measurements has included

- PM1 composition measured with an aerosol chemical speciation monitor (ACSM; Aerodyne, Inc.)
- Hygroscopicity and aerosol size distributions via a tandem differential mobility analyzer (TAMU design)

These measurements complement the collocated measurements of

- cloud condensation nuclei (CCNc; Droplet Measurement Technologies)

and can be used to develop detailed CCN spectra that extrapolate to lower and higher supersaturations. Additional data (e.g., optical properties) are incorporated as checks on derived properties.

We present some initial results from a new effort to produce **CCN spectra by merging these observations**. In addition to providing guidance for modeling efforts, the merged spectra provide insights into seasonal and interannual variations in aerosol types and sources impacting the SGP site.

Field Site Characteristics

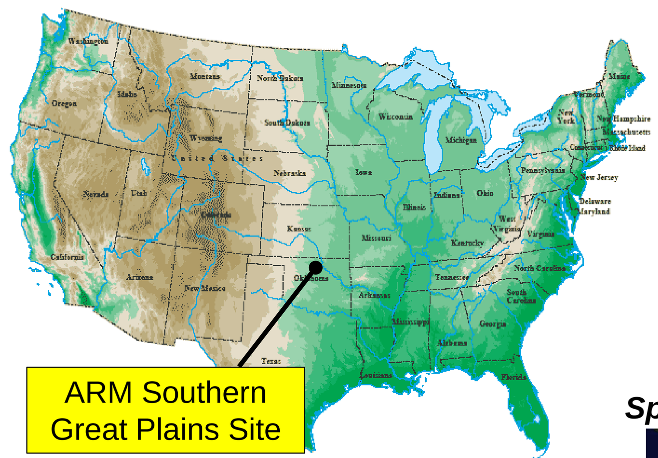

Rural/Agricultural Location

Springtime Sever Weather Potential

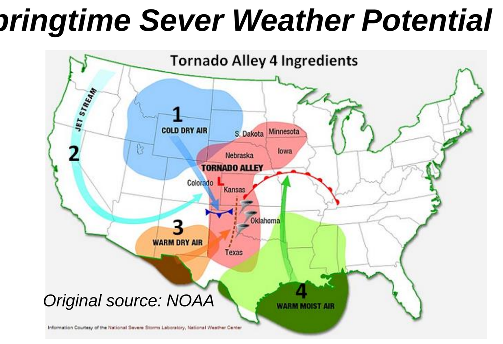

Springtime Biomass Burning Influence

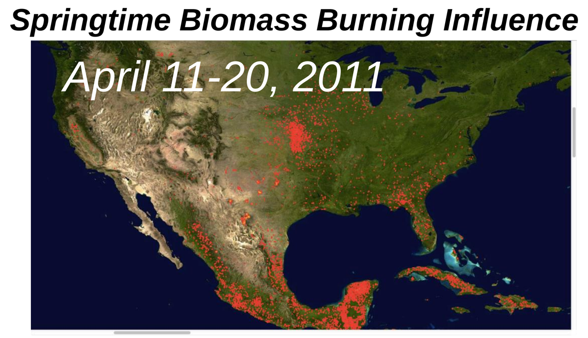

Example map of fire hot spots (MODIS), showing regional agricultural burning and springtime fires in Mexico and C. America.

Seasonal transport patterns

Figures from Andrews et al., *Atmos. Chem. Phys.*, 2011

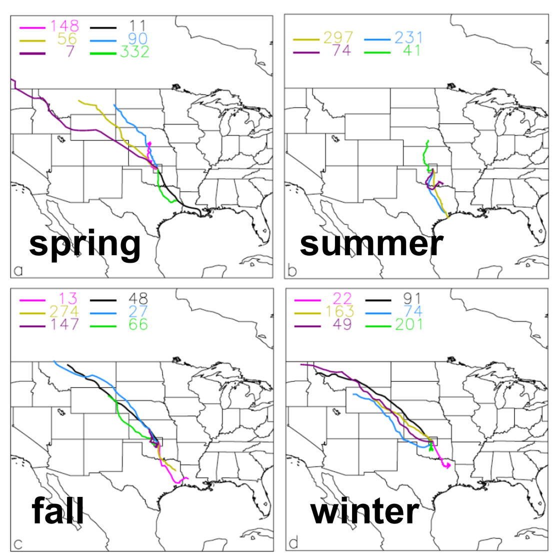

Surface

Figure 1a. *Plots of air mass back trajectory clusters (cluster medians) arriving at 500m to the site (indicated by the square), calculated using NOAA/HYSPLIT. Numbers indicate how many trajectories are in each cluster.*

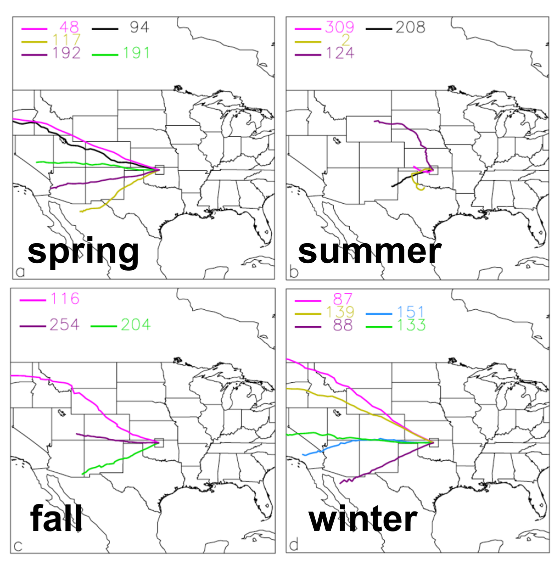

Aloft (3000 m)

Figure 1b. *As in 1a, except for trajectories arriving at 3000m.*

ARM Aerosol Measurements at SGP

Hygroscopic tandem DMA

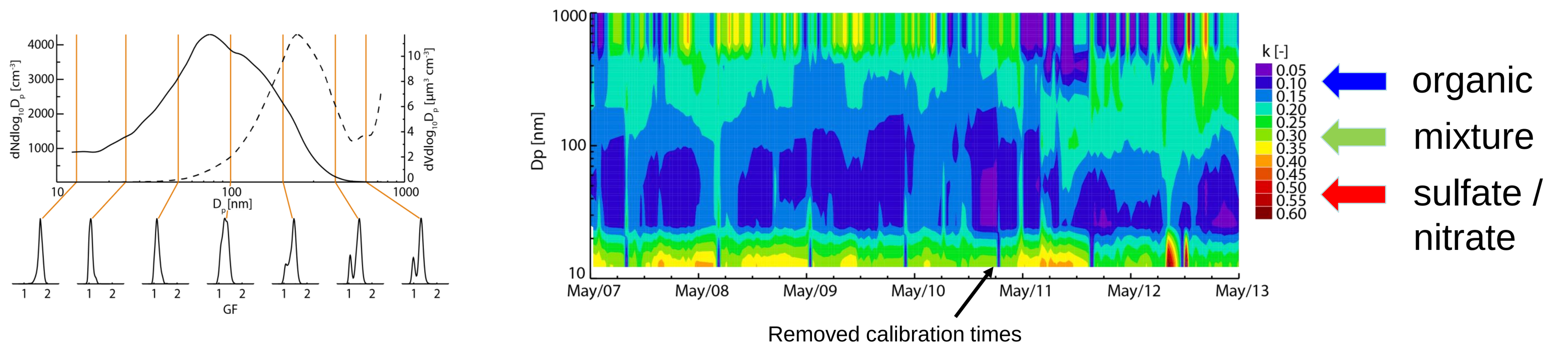

Figure 2. *(left) Example size distribution scan in the HTDMA, showing (lower panel) the distribution of growth factors at the selected sizes. In the right panel, the growth factors have been converted into equivalent hygroscopicity parameters (κ) using Eq. 1 and are shown as a function of particle diameter and time.*

$$\kappa = \frac{(GF^3 - 1)(1 - a_w)}{a_w} \quad \textbf{Eq. 1}$$

Aerosol chemical speciation monitor

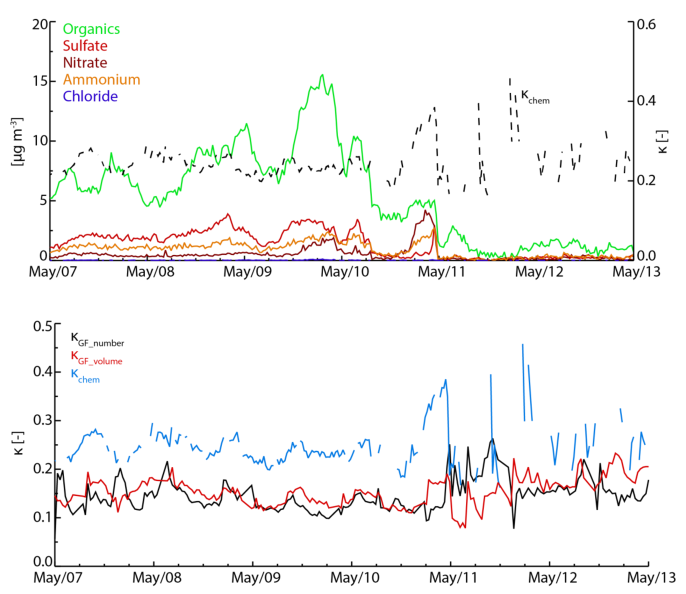

Figure 3. ***(top)*** *Mass concentrations of aerosol chemical species in the PM1 fraction. κ_{chem} is the estimated hygroscopicity based on the observed chemical composition.*

*(**bottom**) A comparison of the hygroscopicity computed from the chemical composition (blue) with that directly measured from the HTDMA. The HTDMA data have been averaged over particle size by weighting by number or volume.*

The overall κ ~ 0.15 is indicative of an organic-dominated sample. The higher values of κ_{chem} indicate the effects of mass weighting, which weights the larger, sulfate-enriched particles more heavily (see Fig. 2).

Number concentrations and size distributions

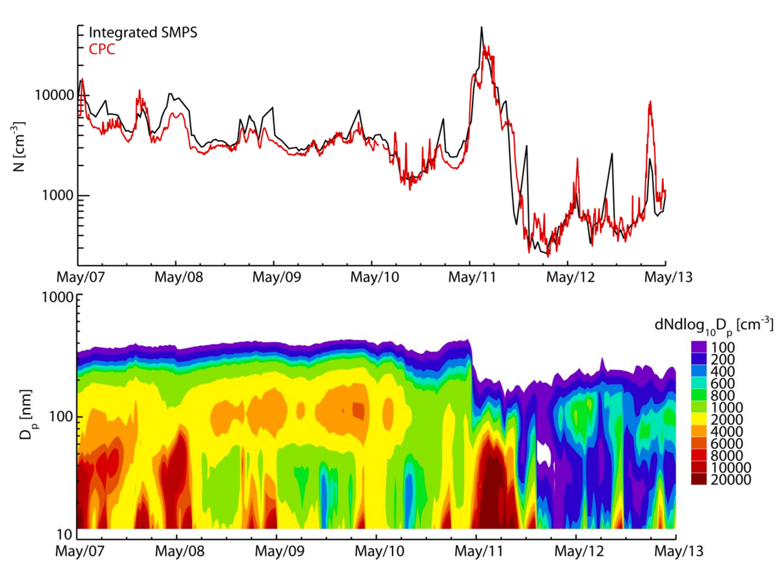

Figure 4. ***(top)****Timeline of total integrated number concentrations from the SMPS, compared with those measured by a CPC. In this time period, there is only a small contribution from ultrafine particles (Dp < 15 nm) not captured by the SMPS scans.* ***(bottom)*** *Contour plot of aerosol number size distributions. Note the presence of a persistent mode near 100 nm of low hygroscopicity (~0.15, Fig. 2), strong incursions of small particles, and a cleanout event toward the end of his period.*

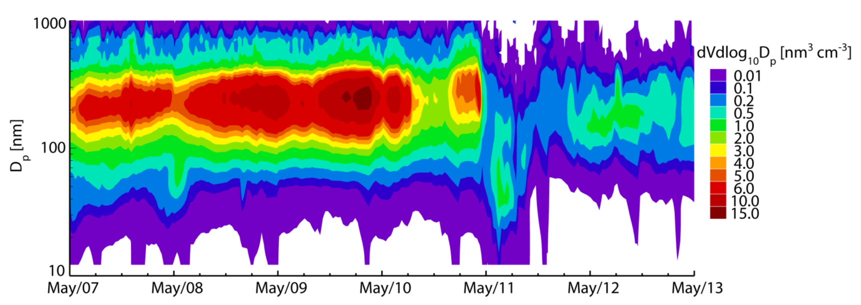

Figure 5. *Timeline of volume distributions (from measured number distributions, Fig. 4). These size distributions correspond most closely to the ACSM measurements. The time period shown in these figures is during the MC3E study, when the site was impacted by intrusions of smoke from fires in Mexico.*

Plans for Product Development and Application

- Additional closure tests are possible with nephelometer data, which help constrain the larger end of the size distribution – generally, CCN active at low supersaturations.
- The algorithms will be applied to multiple years of data at the SGP site, and ultimately expanded to other sites.
- Normalized CCN spectra will be clustered to obtain characteristic spectra, stratified by season and influence (e.g., windblown dust; smoke). The resulting dataset will provide new insights into the sources affecting the SGP aerosol.

Construction of CCN Spectra

	$N_a = f(D_p)$	$+ k_{GF} = f(D_p)$	$+ k_{chem} \neq f(D_p)$	$(N_{CCN})_{calc} = f(S)$ +	N_{CCN} @ $S_1 \ldots S_5$ →	$(N_{CCN})_{BE}$
SGP	SMPS	HTDMA	ACSM, PASS		CCN	

The basic algorithm applied to the data is shown schematically above, for the observations available at the SGP site. Hygroscopicities – either directly measured or inferred from composition – are combined with the size distributions to predict critical supersaturations. The resulting CCN spectra are optimized (adjusting size distributions and/or hygroscopicities) to match (within uncertainties) the CCN concentrations measured directly at the preset supersaturations and are then extrapolated beyond the measurement range of the CCNc.

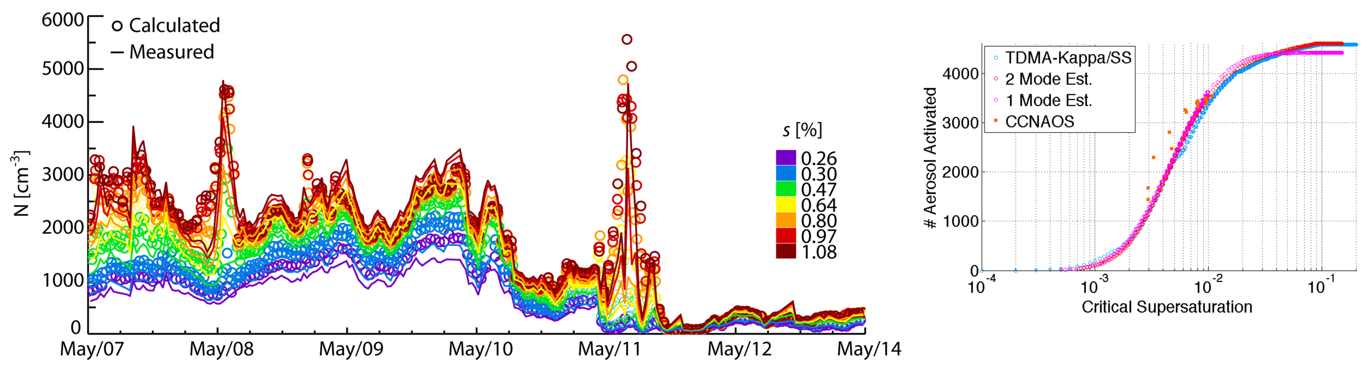

Figure 6. *Example timeline of CCN concentrations as a function of supersaturations (different colors), measured directly (circles) and computed from size distributions and hygroscopicities (lines). Plot at the right shows how the full spectrum is extrapolated across a wide range of supersaturations.*

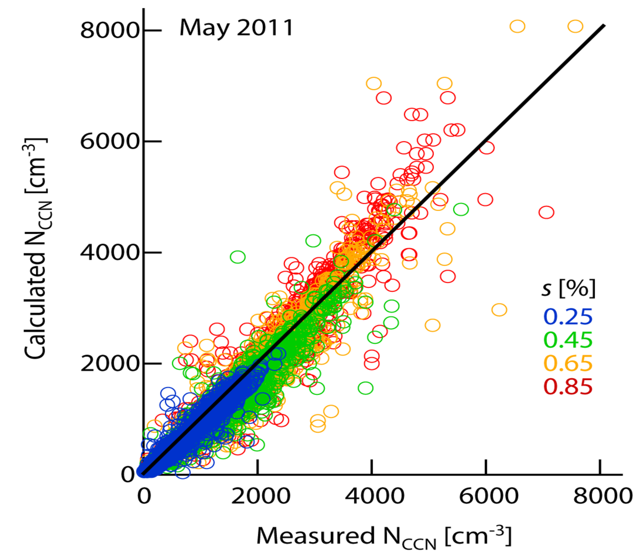

Figure 7. *Closure test of calculated vs. measured CCN at four setpoint supersaturations.*

Best-Estimate CCN Spectra

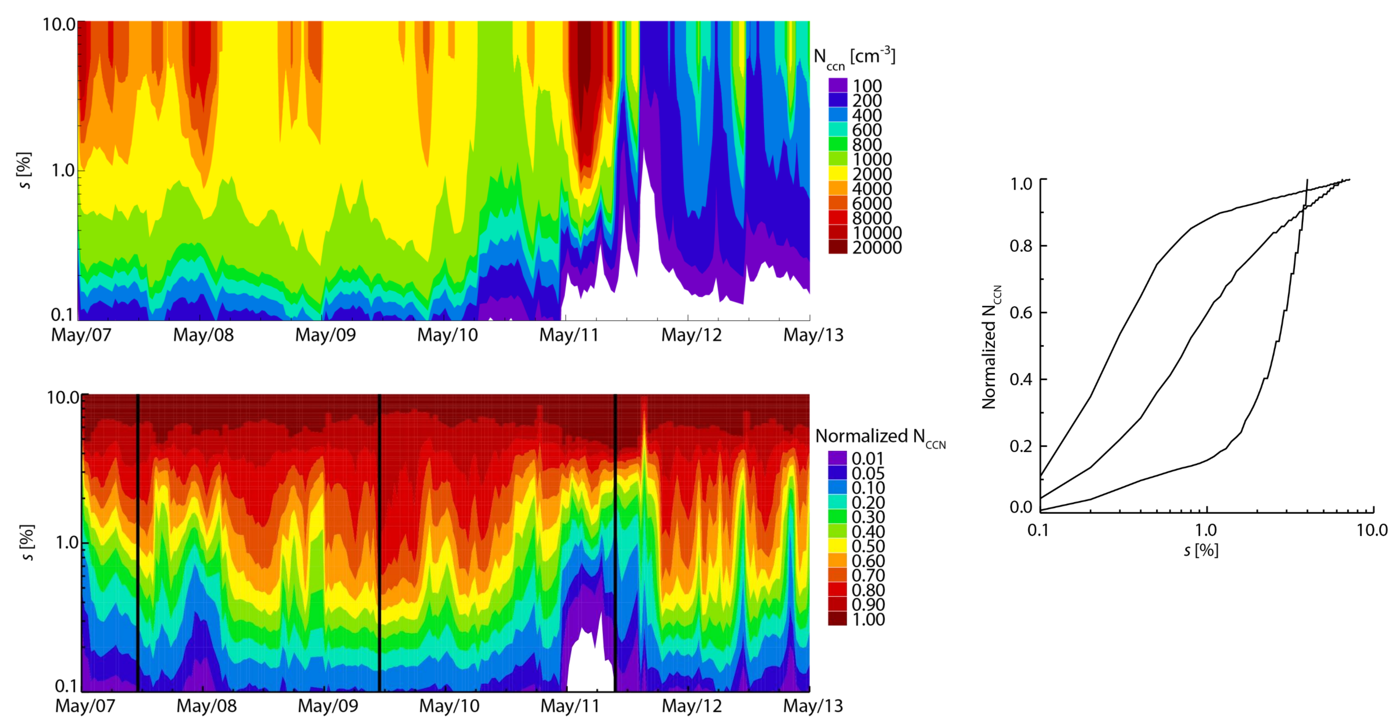

Figure 8. *Contour plot of total (top) and normalized (bottom) best-estimate CCN spectra, spanning up to 10% supersaturation. The higher s values are useful for simulations of deep convection.*

The normalized spectra indicate the presence of several unique CCN types (right) associated with different time periods (black lines in bottom left figure) and meteorological influences. Clustering algorithms will be used to identify these types, and then scaled to absolute values.

Acknowledgment: This work was supported by the Department of Energy under contract DE-SC0016051. The assumptions, findings, conclusions, judgments, and views presented herein are those of the authors and should not be interpreted as necessarily representing DOE policies.